arXiv:1512.03944v1 [cond-mat.mes-hall] 12 Dec 2015

Electron Transport in Molecular Junctions with Graphene as Protecting Layer

Falco Hüser[1,2] and Gemma C. Solomon[1,a)]
[1)] *Nano-Science Center and Department of Chemistry University of Copenhagen, 2100 København Ø, Denmark*
[2)] *Current address: Office for Innovation and Sector Services, Technical University of Denmark, 2800 Kgs. Lyngby, Denmark*

(Dated: 15 December 2015)

We present *ab-initio* transport calculations for molecular junctions that include graphene as a protecting layer between a single molecule and gold electrodes. This vertical setup has recently gained significant interest in experiment for the design of particularly stable and reproducible devices. We observe that the signals from the molecule in the electronic transmission are overlayed by the signatures of the graphene sheet, thus raising the need for a reinterpretation of the transmission. On the other hand, we see that our results are stable with respect to various defects in the graphene. For weakly physiosorbed molecules, no signs of interaction with the graphene are evident, so the transport properties are determined by offresonant tunnelling between the gold leads across an extended structure that includes the molecule itself and the additional graphene layer. Compared with pure gold electrodes, calculated conductances are about one order of magnitude lower due to the increased tunnelling distance. Relative differences upon changing the end group and the length of the molecule on the other hand, are similar.

I. INTRODUCTION

Today, molecular electronics is at a crossroads: While charge transport at the single molecule level has been studied extensively over the past couple of decades both in theory and experiment, the fabrication of efficient and longlasting devices at nanoscale to replace convential semiconductor based electronics seems as out of reach as ever.[1–5] Traditionally, metal electrodes made of gold have been favoured for the design of molecular junctions. Though they provide a suitable test bed for transport measurements and the molecule-metal interface is well understood at the theoretical level, they do not seem viable for practical applications. One fundamental issue is that most fabrication techniques lead to large uncertainties in the junction geometry, resulting in broad variations in measured conductances. This also means that two different junctions are not necessarily comparable (and even less with theoretical models). Furthermore, evaporation of metals onto self-assembled monolayers (SAMs) has turned out to be invasive and can cause short circuits, thus destroying the junction.[6,7] In fact, the device yield with this fabrication technique is very low. Finally, limitations in design in the top-down approaches make new functionalitites difficult to incorporate.

Recently, graphene has been proposed as an alternative soft top contact between SAMs and metal electrodes.[8–11] This material is chemically stable and posesses outstanding electronic and mechanical properties, making it a perfect candidate for durable and reproducible devices. It protects the molecular layer from reorganization and penetration by metal atoms, giving high yield, good operational stability and long device lifetimes. Since graphene is transparent in the range of visible light, it can also be used for optoelectronic molecular switches.[12,13] In addition, the incorporation of a back gate electrode seems achievable. Most importantly, however, from a fundamental point of view is that due to its robustness and flexibility, graphene provides an almost perfect interface.

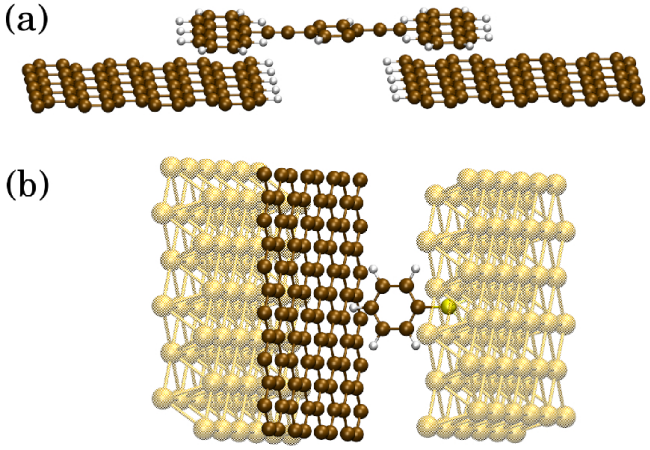

FIG. 1. Comparison of (a) planar molecular junction with graphene nanoribbons as electrodes (b) vertical molecular junction with gold electrodes and graphene as soft top contact layer.

Previous research on molecular junctions including graphene has focused on a lateral device layout using nanoribbons as leads.[14–16] In these junctions, molecules can form covalent C-C bonds with the electrodes allowing for direct injection into the molecular backbone[17,18] or interact via π-π stacking of aromatic rings,[19,20]as sketched in Fig. 1 (a). In a vertical layout, shown in Fig. 1 (b), on the other hand, molecules only physiosorb weakly on the

[a)]Electronic mail: gsolomon@nano.ku.dk

graphene layer and the main interactions are of van-der-Waals type.[21,22] Extensive research has been conducted on the transmission features of molecular junctions with bulk metal electrodes: Polarization and image charge effects lead to a renormalization of the molecular levels and gateway states arise due to hybridization with states located on the end group.[23–26] The level alignment forces the Fermi level of the electrodes, E_F to be located in the gap between the highest occupied and lowest unoccupied molecular orbital (HOMO-LUMO gap) and transport is usually referred to as HOMO- or LUMO-dominated, depending on the exact position of E_F.[27] Whether or not these concepts can be transferred to other junction layouts is not obvious and will be the focus of our discussion.

The transport properties of molecular junctions with graphene as a top contact layer in a vertical device setup have not yet been understood. The questions that we would like to address in this paper are: How do electrons inject from the metal electrode through the graphene into the molecule? What is the signature of the molecule and how does it compare with the well-known case of gold electrodes? And: how stable are results with respect to defects in graphene and variations in the junction geometry?

Even though most experiments are using SAMs, we focus on the transport properties of single molecules in this work. This means that no intermolecular interactions are present, thus allowing for isolating chemical trends from the molecule itself and studying the underlying physics on a basic level.

II. METHOD

The supercell is modelled with 6 by 6 gold atoms in each layer of the electrodes with 7 layers in total. The lattice constant is 4.176 Å. In order to maintain a feasible cell size, the graphene is slightly strechted with a lattice constant of 1.476 Å (this corresponds to a strain of approximately 4 %). In this way, 6×8 elementary unit cells of graphene match with the (111) gold surface. Periodic boundary conditions are applied in all directions. The geometry is shown in Fig. 2 (a) for a Au-graphene-Au junction without molecule. Unless otherwise stated, the distance between the graphene layer and the gold surface is 3.3 Å, as determined in a geometry optimization using the vdW-DF2 functional.[28]

Molecules are placed perpendicularly to the surface with a distance of 2.41 Å to the graphene layer. We note that variations in the position and tilting angle with respect to graphene do not change our results appreciably.

All transport calculations have been performed using a standard nonequilibrium Green's Functions technique based on Density Functional Theory (NEGF-DFT).[29–34] Within the Landauer-Büttiker formalism for coherent transport,[35] the electron conductance at 0 K is given by the value of the transmission, $\tau(E,V)$, at the Fermi level of the electrodes in units of the quantum of conductance, G_0:

$$G = G_0 \, \tau(E, V=0)|_{E=E_F} \, . \tag{1}$$

For numerical stability, we evaluate conductance values by[36]

$$G = G_0 \int dE \, \tau(E) \, (-\partial f(E,T)/\partial E) \, , \tag{2}$$

in steps of 0.01 eV in an energy range from -3 to 3 eV for $T = 300$ K. $f(E,T)$ is the Fermi distribution.

Electronic structures and transmission have been obtained with the GPAW code[37] using the generalized gradient PBE exchange-correlation functional,[38]. We have verified that other functionals, in particular vdW-DF2, do not change the transmission significantly. The choice of the right functional is only an important issue for geometry optimizations. Diffuse basis functions up to double-zeta polarization with a confinement- energy shift of 0.01 eV have been employed.[34] Special care is taken for the k-point sampling in the in-plane directions of the graphene layer, since the transmission turned out to exhibit a strong k-point dependence. A detailed discussion is given in the Supporting Information. The results presented here have been obtained from averaging over $(6 \times 6 \times 1)$ k points.

III. RESULTS

A. Gold-graphene-gold junctions

In order to get a first understanding of our new junction setup, we calculate the vertical transport through a single graphene layer symmetrically sandwiched between the gold electrodes for different distances to the Au surface. The resulting transmission curves are shown in Fig. 2 (b). First, we notice that the signal is not entirely smooth but exhibits a series of sharp resonances. This is a consequence of the finite k-point sampling in our calculations.[39,40] Nonetheless, they clearly demonstrate the presence of graphene states, which are uncoupled or only very weakly coupled to the gold leads. For an infinite number of k points, the resonances are expected to average out. The overall properties of the transmission are a very high and broad peak around -2.3 eV relative to the Fermi level, a smaller split peak at -1.3 eV and increasing values up to 2 eV (see the Supporting Information for more details). Around the Fermi level, the transmission is rather flat. By increasing the distance to the gold surface, the conductance drops off by several orders of magnitude, in agreement with a model for offresonant tunnelling between the gold leads.

In Fig. 2 (c), we compare the transmission for monolayer, bilayer and trilayer graphene with an interlayer separation of 3.35 Å (as in bulk graphite) and 3.3 Å distance to the gold surfaces on both sides. More peaks appear for additional layers, due to the higher number of

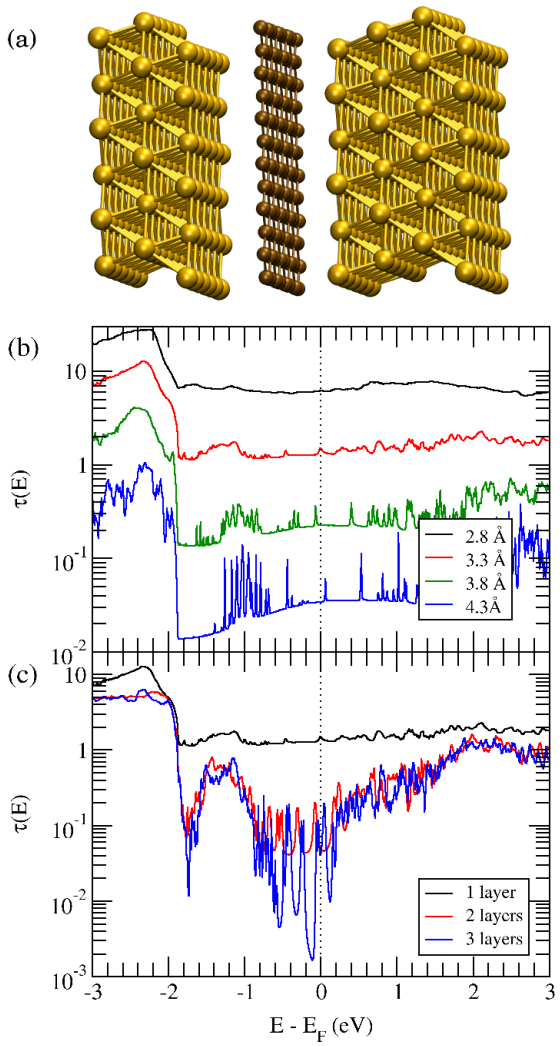

FIG. 2. (a) Schematic junction geometry showing all atoms of the unit cell. Vertical transmission for gold-graphene-gold junctions with (b) varying distance and (c) different number of graphene layers.

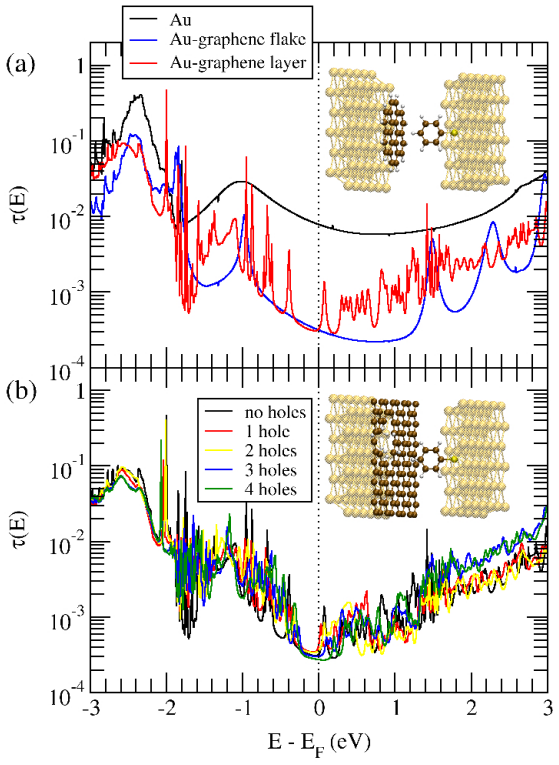

FIG. 3. Transmission through (a) a benzene-thiol with gold leads only, an additional graphene flake and an additional perfect graphene monolayer and (b) a benzene-thiol with a graphene monolayer including hole defects. Inset: Schematic junction geometry with (a) graphene flake and (b) 4 holes.

electronic states. However, inbetween the resonances, the transmission decays exponentially with increasing thickness, corresponding to an increase of the tunnelling distance.

B. Introducing graphene defects

Using the example of a benzene-thiol molecule, we investigate the influence of defects in the graphene layer. On the right side, the benzene is attached to the gold electrode with a thiol end group binding to three Au atoms in a fcc hollow site. Fig. 3 (a) shows the calculated transmission curves for a junction consisting of the molecule with gold electrodes only, an additional graphene flake (consisting of 7 rings and passivated at the edges), and an additional perfect graphene monolayer. The distance between the molecule and either the left gold electrode or the graphene is 2.41 Å in all cases. The black line (no graphene) shows the typical sulfur-induced resonance around 1 eV below the Fermi level. Its height is reduced due to the asymmetric coupling. Upon adding the graphene flake between the molecule and the left electrode, the transmission drops by one order of magnitude. The peak at −1 eV becomes sharper due to a weakened interaction with the gold electrode and further resonances appear. The overall shape of the transmission, however, is not altered significantly. This also holds when a perfect graphene monolayer is inserted between the benzene-thiol and the left electrode. However, the signals are obstructed by the features of the graphene itself. By simply looking at the transmission, it is not clear what comes from the molecule and what from the graphene. They cannot be separated.

As another type of defect, we introduce holes in the graphene layer by removing 1 to 4 adjacent carbon atoms and passivating undercoordinated atoms at the emerging edges. As plotted in Fig. 3 (b), the resonance peaks move in energy (in accordance with a change in the density of

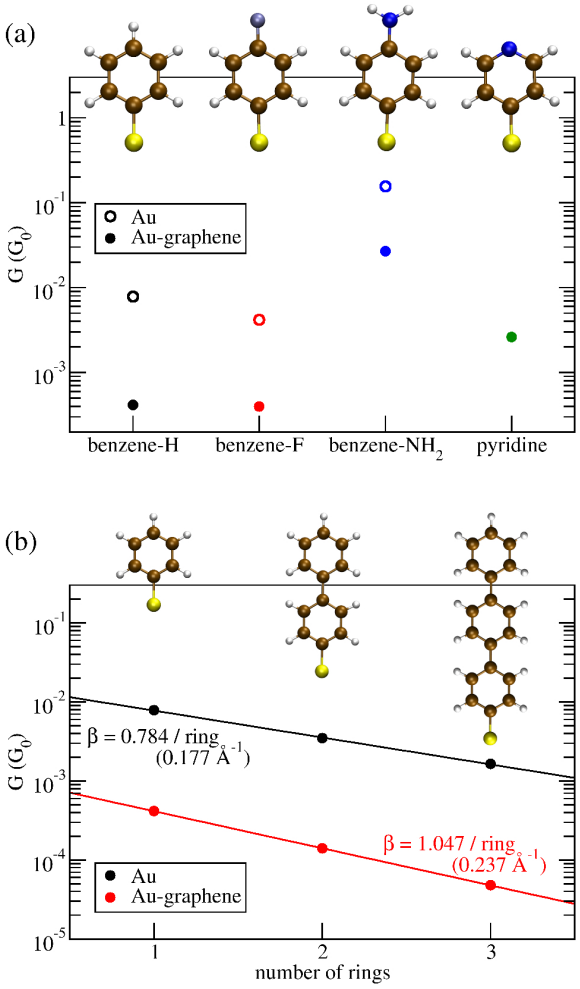

FIG. 4. Conductance for (a) benzene-thiol with 3 different end groups and pyridine-thiol and (b) N-phenylenethiols ($N = 1, 2, 3$) and fitted values for the exponential decay factor, β.

states of the graphene), whereas the value of the conductance and the curvature in the vicinity of the Fermi level roughly remain stable.

Finally, we have varied the number of graphene layers. The observations are similar to what is described for Fig. 2 (c) in the previous section for the case without molecule: A larger number of sharp resonances, a reduction of the gap and a drastic lowering of the transmission in the gap. The corresponding transmissions can be found in the Supporting Information.

C. Varying the end group

For the gold-graphene-molecule-gold junction with a perfect graphene monolayer, we explore the effect of different end groups on the transport properties and thus the molecule-graphene interaction. The results are plotted in Fig. 4 (a) for benzene-thiols with three different terminating groups on the graphene side (hydrogen, fluorine and amine) and for pyridine-thiol. First, we note that the corresponding transmissions (see Supporting Information) for hydrogen and fluorine end groups are almost identical. This indicates a very weak interaction. The two molecules are of the same size and the conductance seems to be defined by the distance to the gold electrode. For the amine end group, we see a broad resonance right below the Fermi level. This arises from a conducting orbital formed by the nitrogen p_z orbital and the π-system of the benzene ring. The conductance is much higher than for the other molecules. It is important to point out that, also here, the overall shape of the transmission curves is the same as for the case of bare gold electrodes, but shifted to lower values and superposed by the graphene signal.

Pyridine is a much shorter molecule and has a larger conductance than benzene-thiol with hydrogen and fluorine end groups. As for those two molecules, there does not seem to be a conducting molecular orbital present in the vicinity of the Fermi level. The level of "background noise" from graphene states is the same in all cases. In fact, single resonances show up at the same energies as for the junctions with a single graphene layer only (and no molecule).

The relative differences in the conductance are about the same for the two different junction setups. However, there are apparent differences in the curvature of the transmission around E_F. This can be seen as a signature of the molecule (including the end group).

For benzene-thiol with amine end group, we have also calculated the transmission for increasing distances between the molecule and the graphene layer. The only difference that we observe is a constant decrease, while its shape remains unchanged (equivalent to Fig. 2 (b)). This is another indication for that there are no apparent interactions.

D. Length dependence

A well known characteristic of a molecular wire is the exponential decay of the conductance with length.[41] In Fig. 4 (b), we compare the length dependence for phenylenethiols with gold and gold-graphene electrodes. The data points are fitted to an exponential function. The obtained decay factors, β, are $0.18\,\text{Å}^{-1}$ and $0.24\,\text{Å}^{-1}$, respectively. This is a small but nonetheless apparent difference. However, we note that due to the ragged structure of the transmission curves, the determination of the conductance values is sensitive to numerical errors. Still, the qualitative picture remains.

IV. CONCLUSIONS

It is obvious that transport through vertical devices including graphene layers differs substantially from that of gold-molecule-gold junctions. The appearance of graphene signals in the whole energy range of the transmission makes it difficult to identify signatures of the molecule itself. The classical picture of HOMO- or LUMO-dominated transport does not seem to hold. Instead, one may think of the graphene layer as behaving like a large molecule itself and the signatures present in the transmission are those of both the molecule and the graphene.

We note that the transmission has a very strong k-point dependence with distinct, very sharp peaks for different k points. Upon proper averaging, their height is reduced and the transmission becomes smoother. For finite k-point samplings, they cause a background noise signal. It is therefore more meaningful to look at the conductance (evaluated for finite temperatures by Eq. (2)) and relative differences only.

For weakly physiosorbed molecules, no signs of interactions with the graphene layer can be seen. The overall shape of the transmission, in particular the curvature is not changed compared with junctions with gold only. This is best seen in Fig. 3 (a) for going from no graphene to a finite flake and finally to an infinite layer. Relative differences upon changing the chemistry and length of the molecule are very similar.

In all cases, we see a drastic reduction of the conductance in agreement with an increase of the tunnelling distance from gold to gold electrode. All our observations hold when defects in the graphene are present. Measurements on molecular junctions with a graphene top layer should therefore give very stable results. Relative changes in conductance should be comparable to junction with gold only.

For further understanding of the transport properties and exploration of the transmission, measurements of $I-V$ curves and the thermopower might be very helpful. Since the thermopower is proportional to the slope of the transmission, it is much more sensitive to the presence and position of sharp peaks close to the Fermi level. From our calculations, it was not possible to extract numerically reliable values. Measured values, on the other hand, could give valuable information on the nature of electron transport in the molecular junctions and reveal trends across different classes of molecules that are not available from the conductance only.[26,42] For the thermopower, larger and also qualitative differences can be expected compared to regular gold-molecule-gold junctions.

V. ACKNOWLEDGEMENTS

This project has received fundings from the European Research Council under the European Union's (EU) Seventh Framework Program (FP7/2007-2013)/ERC Grant Agreement No. 258806.

VI. SUPPORTING INFORMATION

The Supporting Information includes a detailed discussion of the k-point sampling used in the calculation of averaged transmission curves as well as transmissions for all molecules of this study.

[1] H. Song, M. A. Reed, and T. Lee, "Single molecule electronic devices." Adv. Mater. Weinheim **23**, 1583–608 (2011).
[2] M. Kiguchi and S. Kaneko, "Single molecule bridging between metal electrodes." Phys Chem Chem Phys **15**, 2253–67 (2013).
[3] L. Sun, Y. A. Diaz-Fernandez, T. A. Gschneidtner, F. Westerlund, S. Lara-Avila, and K. Moth-Poulsen, "Single-molecule electronics: from chemical design to functional devices." Chem Soc Rev **43**, 7378–411 (2014).
[4] F. Schwarz and E. Lörtscher, "Break-junctions for investigating transport at the molecular scale." J Phys Condens Matter **26**, 474201 (2014).
[5] R. J. Nichols and S. J. Higgins, "Single-molecule electronics: Chemical and analytical perspectives." Annu Rev Anal Chem (Palo Alto Calif) **8**, 389–417 (2015).
[6] B. de Boer, M. M. Frank, Y. J. Chabal, W. Jiang, E. Garfunkel, and Z. Bao, "Metallic contact formation for molecular electronics: interactions between vapor-deposited metals and self-assembled monolayers of conjugated mono- and dithiols," Langmuir **20**, 1539 (2004).
[7] C. N. Lau, D. R. Stewart, R. S. Williams, and M. Bockrath, "Direct observation of nanoscale switching centers in metal/molecule/metal structures," Nano Letters, vol. 4, issue 4, pp. 569-572 **4**, 569–572 (2004).
[8] G. Wang, Y. Kim, M. Choe, T.-W. Kim, and T. Lee, "A new approach for molecular electronic junctions with a multilayer graphene electrode." Adv. Mater. Weinheim **23**, 755–60 (2011).
[9] T. Li, J. R. Hauptmann, Z. Wei, S. Petersen, N. Bovet, T. Vosch, J. Nygård, W. Hu, Y. Liu, T. Bjørnholm, K. Nørgaard, and B. W. Laursen, "Solution-processed ultrathin chemically derived graphene films as soft top contacts for solid-state molecular electronic junctions." Adv. Mater. Weinheim **24**, 1333–9 (2012).
[10] S. Petersen, M. Glyvradal, P. Bøggild, W. Hu, R. Feidenhans'l, and B. W. Laursen, "Graphene oxide as a monoatomic blocking layer." ACS Nano **6**, 8022–9 (2012).
[11] S. Parui, L. Pietrobon, D. Ciudad, S. Vélez, X. Sun, F. Casanova, P. Stoliar, and L. E. Hueso, "Gate-controlled energy barrier at a graphene/molecular semiconductor junction," Advanced Functional Materials **25**, 2972 (2015).
[12] S. Seo, M. Min, S. M. Lee, and H. Lee, "Photo-switchable molecular monolayer anchored between highly transparent and flexible graphene electrodes," Nature Communications, Volume 4, id. 1920 (2013). **4**, 1920 (2013).
[13] T. Li, M. Jevric, J. R. Hauptmann, R. Hviid, Z. Wei, R. Wang, N. E. A. Reeler, E. Thyrhaug, S. Petersen, J. A. S. Meyer, N. Bovet, T. Vosch, J. Nygård, X. Qiu, W. Hu, Y. Liu, G. C. Solomon, H. G. Kjaergaard, T. Bjørnholm, M. B. Nielsen, B. W. Laursen, and K. Nørgaard, "Ultrathin reduced graphene oxide films as transparent top-contacts for light switchable solid-state molecular junctions." Adv. Mater. Weinheim **25**, 4164–70 (2013).
[14] X. Zheng, S.-H. Ke, and W. Yang, "Conductive junctions with parallel graphene sheets." J Chem Phys **132**, 114703 (2010).
[15] D. Carrascal, V. M. García-Suárez, and J. Ferrer, "Impact of edge shape on the functionalities of graphene-based single-molecule electronics devices," Physical Review B, vol. 85, Issue 19, id. 195434 **85**, 195434 (2012).

[16]B. D. Fainberg, "Photon-assisted tunneling through molecular conduction junctions with graphene electrodes," Physical Review B, Volume 88, Issue 24, id.245435 **88**, 245435 (2013).
[17]B. K. Nikolić, K. K. Saha, T. Markussen, and K. S. Thygesen, "First-principles quantum transport modeling of thermoelectricity in single-molecule nanojunctions with graphene nanoribbon electrodes," Journal of Computational Electronics **11**, 78 (2012).
[18]Y. Cao, S. Dong, S. Liu, Z. Liu, and X. Guo, "Toward functional molecular devices based on graphene-molecule junctions." Angew. Chem. Int. Ed. Engl. **52**, 3906–10 (2013).
[19]F. Prins, A. Barreiro, J. W. Ruitenberg, J. S. Seldenthuis, N. Aliaga-Alcalde, L. M. K. Vandersypen, and H. S. J. van der Zant, "Room-temperature gating of molecular junctions using few-layer graphene nanogap electrodes." Nano Lett. **11**, 4607–11 (2011).
[20]K. Ullmann, P. B. Coto, S. Leitherer, A. Molina-Ontoria, N. Martín, M. Thoss, and H. B. Weber, "Single-molecule junctions with epitaxial graphene nanoelectrodes." Nano Lett. **15**, 3512–8 (2015).
[21]M. Hassan, M. Walter, and M. Moseler, "Interactions of polymers with reduced graphene oxide: van der waals binding energies of benzene on graphene with defects," Physical Chemistry Chemical Physics, vol. 16, issue 1, p. 33 **16**, 33 (2014).
[22]P. L. Silvestrelli and A. Ambrosetti, "Including screening in van der waals corrected density functional theory calculations: The case of atoms and small molecules physisorbed on graphene," The Journal of Chemical Physics, Volume 140, Issue 12, id.124107 **140**, 124107 (2014).
[23]J. B. Neaton, M. S. Hybertsen, and S. G. Louie, "Renormalization of molecular electronic levels at metal-molecule interfaces," Physical Review Letters, vol. 97, Issue 21, id. 216405 **97**, 216405 (2006).
[24]G. Peng, M. Strange, K. S. Thygesen, and M. Mavrikakis, "Conductance of conjugated molecular wires: Length dependence, anchoring groups, and band alignment," The Journal of Physical Chemistry C **113**, 20967 (2009).
[25]G. Heimel and J.-L. Brédas, "Molecular electronics: Reflections on charge transport," Nature Nanotechnology, Volume 8, Issue 4, pp. 230-231 (2013). **8**, 230–231 (2013).
[26]F. Hüser and G. C. Solomon, "From chemistry to functionality: Trends for the length dependence of the thermopower in molecular junctions," The Journal of Physical Chemistry C , 150612131913005 (2015).
[27]J. B. Neaton, "Single-molecule junctions: thermoelectricity at the gate." Nat Nanotechnol **9**, 876–7 (2014).
[28]K. Lee, É. D. Murray, L. Kong, B. I. Lundqvist, and D. C. Langreth, "Higher-accuracy van der waals density functional," Physical Review B, vol. 82, Issue 8, id. 081101 **82**, 081101 (2010).
[29]J. Taylor, H. Guo, and J. Wang, "Ab initio modeling of quantum transport properties of molecular electronic devices," Physical Review B, vol. 63, Issue 24, id. 245407 **63**, 245407 (2001).
[30]Y. Xue, S. Datta, and M. A. Ratner, "First-principles based matrix green's function approach to molecular electronic devices: general formalism," Chemical Physics, Volume 281, Issue 2, p. 151-170. **281**, 151–170 (2002).
[31]M. Brandbyge, J.-L. Mozos, P. Ordejón, J. Taylor, and K. Stokbro, "Density-functional method for nonequilibrium electron transport," Physical Review B, vol. 65, Issue 16, id. 165401 **65**, 165401 (2002).
[32]K. S. Thygesen, M. V. Bollinger, and K. W. Jacobsen, "Conductance calculations with a wavelet basis set," Physical Review B, vol. 67, Issue 11, id. 115404 **67**, 115404 (2003).
[33]M. Strange, I. S. Kristensen, K. S. Thygesen, and K. W. Jacobsen, "Benchmark density functional theory calculations for nanoscale conductance." J Chem Phys **128**, 114714 (2008).
[34]M. Strange, C. Rostgaard, H. Häkkinen, and K. S. Thygesen, "Self-consistent gw calculations of electronic transport in thiol- and amine-linked molecular junctions," Physical Review B, vol. 83, Issue 11, id. 115108 **83**, 115108 (2011).
[35]Y. Meir and N. S. Wingreen, "Landauer formula for the current through an interacting electron region," Physical Review Letters, Volume 68, Issue 16, April 20, 1992, pp.2512-2515 **68**, 2512–2515 (1992).
[36]F. Pauly, J. K. Viljas, and J. C. Cuevas, "Length-dependent conductance and thermopower in single-molecule junctions of dithiolated oligophenylene derivatives: A density functional study," Physical Review B, vol. 78, Issue 3, id. 035315 **78**, 035315 (2008).
[37]J. Enkovaara, C. Rostgaard, J. J. Mortensen, J. Chen, M. Dułak, L. Ferrighi, J. Gavnholt, C. Glinsvad, V. Haikola, H. A. Hansen, H. H. Kristoffersen, M. Kuisma, A. H. Larsen, L. Lehtovaara, M. Ljungberg, O. Lopez-Acevedo, P. G. Moses, J. Ojanen, T. Olsen, V. Petzold, N. A. Romero, J. Stausholm-Møller, M. Strange, G. A. Tritsaris, M. Vanin, M. Walter, B. Hammer, H. Häkkinen, G. K. H. Madsen, R. M. Nieminen, J. K. Nørskov, M. Puska, T. T. Rantala, J. Schiøtz, K. S. Thygesen, and K. W. Jacobsen, "Electronic structure calculations with gpaw: a real-space implementation of the projector augmented-wave method." J Phys Condens Matter **22**, 253202 (2010).
[38]J. P. Perdew, K. Burke, and M. Ernzerhof, "Generalized gradient approximation made simple," Physical Review Letters, Volume 77, Issue 18, October 28, 1996, pp.3865-3868 **77**, 3865–3868 (1996).
[39]K. S. Thygesen and K. W. Jacobsen, "Interference and k -point sampling in the supercell approach to phase-coherent transport," Physical Review B, vol. 72, Issue 3, id. 033401 **72**, 033401 (2005).
[40]J. T. Falkenberg and M. Brandbyge, "Simple and efficient way of speeding up transmission calculations with k-point sampling." Beilstein J Nanotechnol **6**, 1603–8 (2015).
[41]M. Magoga and C. Joachim, "Conductance and transparence of long molecular wires," Physical Review B (Condensed Matter), Volume 56, Issue 8, August 15, 1997, pp.4722-4729 **56**, 4722–4729 (1997).
[42]O. Karlström, M. Strange, and G. C. Solomon, "Understanding the length dependence of molecular junction thermopower," The Journal of Chemical Physics, Volume 140, Issue 4, id.044315 **140**, 044315 (2014).